

DOI: 10.24425/amm.2020.131751

W. OSUCH¹, R. BŁONIAZ^{1*}, G. MICHTA¹, I. SULIGA¹

EVOLUTION OF THE DISLOCATION STRUCTURE OF IRON METEORITE

The state of the dislocation substructure of meteorite in which the history of phenomena accompanying the meteorite during its passage through the Earth's atmosphere is recorded remains unused. The main goal of the presented work is a comprehensive analysis of the dislocation structure of the iron meteorite from the Morasko reserve (Poland, Wielkopolska Voivodeship) by TEM methods to determine the conditions and mechanism of its formation. The work is cognitive in the field of phenomena related to the destruction and deformation of the material in extreme conditions: space and terrestrial space. It can also be useful in the research on the creation of the material with specific mechanical properties, as well as a unique reference material for earth experiments with low-temperature deformation, high-speed deformation, recrystallization processes with short thermal pulses and structure relaxation in conditions of very long time periods.

Keywords: iron meteorite, Morasko, TEM study, dislocation structure, Neumann's bands

1. Introduction

Falling meteorites terrified people, but simultaneously they fascinated with their properties. They became a synonym of the power of rulers, they had magical power, but also simple tools and ornaments were made of them. Archeology known are iron objects from thousands of years ago characterized by nickel content, whose origin is attributed to meteorites [1-4]. Iron meteorites were probably the prototype of nickel steels, the first alloy steels [5], in which a wide spectrum of structures and mechanical properties were obtained by combining contents of Ni and C. Contemporary attempts at processing of meteoritic material by hot forging of meteoric material confirm the possibility of its practical use [6-7].

Meteorites are the subject of meteoritic studies conducted by cosmologists, mineralogists and physicists. Inventory of findings, their classification, performs full chemical, mineralogical and structural characteristics. Places of origin, time and conditions for their formation in outer space are considered, as well as the date of meteorites' fall to the surface of the Earth. The material aspect of these peculiar materials is neglected, and for material scientists, meteorites are a unique reference material for earth experiments with low-temperature deformation, high-speed deformation, recovery processes with short thermal pulses and structure relaxation in very long time periods.

There are four classification groups of meteorites: chondrites, achondrites, stone – iron and iron [8]. A characteristic feature of the group of iron meteorites is the specific chemical composition: Fe, Ni, Co, P, S, C and, consequently, the mineralogical composition. In a set of 549 iron meteorites registered until mid – XIX – mid. twentieth century [8] content of main chemical components: Ni and P, varies respectively within the range: 6.51-8.53%, and 0.12-0.39%. Detailed contents of the basic alloying elements are presented in the diagrams (Fig. 1). Three iron meteorite kinds can be distinguished. Over half had a Ni content below 7%, ¼ – between 7-8% and ¼ above 8%. Phosphorus content has a statistical spread of 0.1-3% and its content is unrelated to Ni. Apart from the other chemical components, iron meteorites are alloys from the Fe-Ni system. It is a system with the so-called open austenite field. Fe-Ni alloys may have the α (nickel ferrite) structure, γ (nickel austenite), or $\alpha + \gamma$ mixture. The meteorites of the analyzed group, without taking into account the influence of pressure, should have the structure α or $\alpha + \gamma$. In mineralogical terminology, nickel ferrite α is called kamacite and nickel austenite γ -taenite. In some cases, kamacite and taenite form a characteristic mixture called plessite. Phosphorus is present in a solution in ferrite and in the form of iron-nickel phosphides (Fe, Ni)₃P. There are two morphological variations of phosphides: rhabdite and schreibersite. Rhabdite is a crystalline form of iron-nickel phosphide distributed statisti-

¹ AGH UNIVERSITY OF SCIENCE AND TECHNOLOGY, FACULTY OF METALS ENGINEERING AND INDUSTRIAL COMPUTER SCIENCE, AL. MICKIEWICZA 30, 30-059 KRAKÓW, POLAND

* Corresponding author: bloniarz@agh.edu.pl



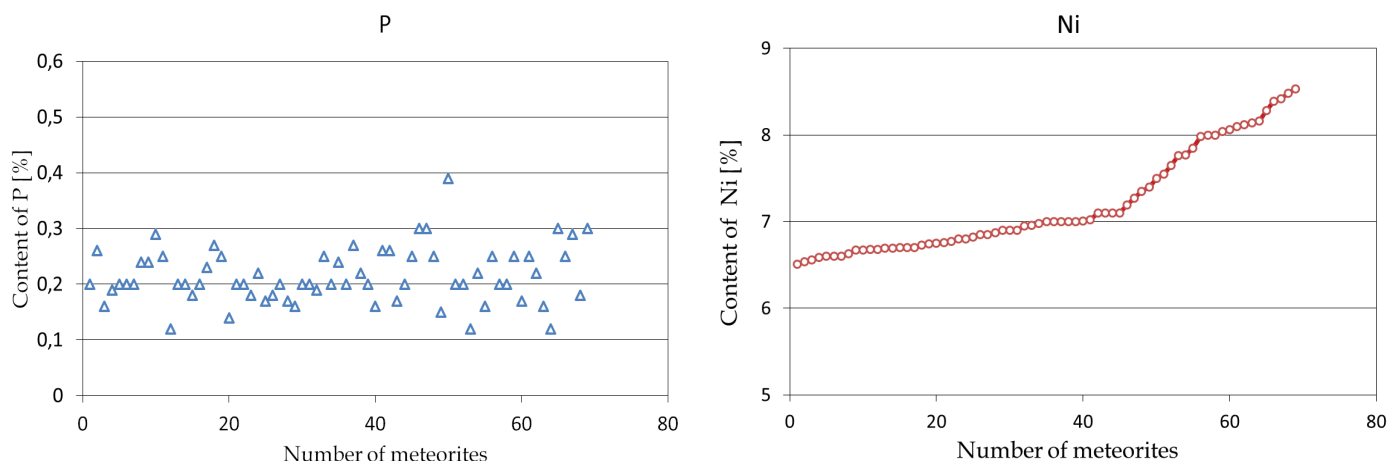


Fig. 1. Ni and P in meteorites collected during the mid nineteenth – mid. twentieth century [8]

cally inside the matrix of kamacite, schreibersite has the form of phosphorus eutectic $\alpha - (\text{Fe}, \text{Ni})_3\text{P}$ in intergranular spaces. The other chemical elements forms precipitations as: graphite, silicate, morphologically related to schreibersite-troilite FeS and cohenite $(\text{Fe}, \text{Ni})_3\text{C}$.

Structural investigations of iron meteorites led to the definition of certain typological classes of iron meteorites, of which those with a ferritic structure are called hexaedrites, austenitic structure – ataxites, while octahedrites are characterized by a mixture of these two phases. The dominant structural class among octahedrites is Medium Octahedrites (Om class), often Coarse Octahedrites (Og class) [8].

A characteristic feature of the structure of iron meteorites is grain size coarseness and structural heterogeneity. The structure is shaped in extremely different conditions. The primary and secondary structure are considered. Two approaches of primary meteor's structure forming are considered – either through a crystallization from homogeneous liquid from the Fe-Ni system with admixtures, crystallizing with very small undercooling, or through sintering material from parent metals and elements of pollution.

During the cooling of the shaped high-temperature taenite phase, non-metallic inclusions crystallize in the inter-crystalline spaces: phosphates and sulphides. After undercooling below the equilibrium line, the transformation $\gamma - \alpha$ begins. Crystallization of taenite and subsequent conversion of $\gamma - \alpha$ takes place under conditions of extremely slow cooling, on the order of $0.5\text{-}5000^\circ\text{C}/10^6$ years. In space, the only form of heat exchange is radiation. The structural effect of cooling will be determined by the chemical homogeneity of the meteorite, thermal conductivity, position relative to the stars emitting heat radiation, cosmic radiation, collision energy. As a consequence, Widmanstätten structure, even-axial or lamellar structure will be formed.

Buchwald [8] lists 4 mechanisms of forming the secondary structure of iron meteorites: plastic deformation, solid phase transformation, remelting, annealing.

As a result of collision (preatmospheric shock-deformation), or under the influence of atmospheric pressure, there may be a cold plastic deformation. The deformation is expressed by the

increasing the density of dislocations in both metallic phases and twins in kamacite, and the minerals are deformed or crushed.

In the first studies of the dislocation structure of the meteorite, a density of dislocations of approx. $10^6/\text{cm}^2$ was found in kamacite at a hardness of 250 HV [9]. Dislocations form clusters and networks. As a result, the kamacite reinforcement in the meteorite with 7% Ni content in the original state has a hardness of about 155 HV, and after deformation about 325HV [8]. The formation of twins is favored by a pressure shock above 1 GPa, and their density depends on the pressure. Deformation of taenite can result in a significant increase in hardness to approx. 475HV, as a result of carbon supersaturation and martensitic transformation. A very high pressure shock above 13 GPa can lead to the formation of a high-density hexagonal variant $\epsilon\text{-Fe}$, which after pressure relief undergoes martensitic transformation [10], the triple point of the system has the coordinates: 510°C and 11.2 GPa.

In analogous conditions: in the outer space, in orbit, during the fall and formation of the crater, the secondary structure of meteorites is formed. The formation of the structure is accompanied by thermal effects related to earlier deformations. Generally, the phenomena occurring in the deformed material are comparable to long-term recrystallization of the deformed material at temperatures close to the recrystallization temperature, what results in effect of polygonisation and primary recrystallization.

Modern science and research methodology increase the possibilities to describe structure of meteorite. An important role is played here, beginning with the classic work [11], TEM methods [12]. In the interpretation of research results, one aspect of the projection of a meteorite structure for modern materials is neglected. For this, certain simplifications in the scope of meteorite research and their reconciliation with commonly used earth materials research are necessary, which were attempted in this work.

2. Subject and methodology of research

The research was carried out on samples taken from a meteorite weighing 260 g provided by Mr. Krzysztof Socha.

The meteorite was found in the Morasko reserve. Meteorites Morasko craters were discovered in 1914. On an elliptical surface of 1.4-0.3 km, 8 craters with a diameter of 25-60 m were identified. Catalog structural studies were carried out on 2 meteorites weighing 78 kg and dimensions 50×30×15 cm [13]. Widmanstätten structures with 2.5 mm lamellar and grain structure with Neumann bands were revealed. The share of taenite and plessite was estimated at approx. 2-3%. Some of the plessite fields were soiled and cut, which is evidence of the meteor fragmentation. In addition, schreibersite was found at the grain boundaries of the matrix, in the form of 1-3 mm layers, 5-10 μm rhabdite and troilite in subsurface zones. Cohenite (Fe, Ni)₃C was locally observed in the form of 50-300 μm precipitates. On a smaller 200 g meteorite from this crater, the transformation of kamacite into α₂ and crystallization of cohenite were found. Morasko meteorites were classified as coarse (inclusion-rich) octahedrite, structural class Og; Bandwidth 1.5±0.5 mm, Neumann bands, type member Canyon Diablo [8]. The catalog chemical composition is: 6.70% Ni, 0.53% Co, 0.18% P. Neumann bands, kamacite (α phase) and a thick rind shell were identified in the structure. The studies on the structure and properties of the Morasko craters have been reported, among others, in the works [14-15].

Fig. 2 shows the examined meteorite and its cross-section, with the location of sampling for TEM testing. The average size of fragments is approx. 20 mm. In each of them, 3-6 grains are observed, divided into twin bands.

The Morasko meteorite fragment extracted for TEM studies had dimensions 45×35×20 mm and the following chemical composition: Fe-92.2%, Ni-6.75%, Co-0.53%, P-0.18%, Cu-0.15%, C-0.02%, Ge-0.05%. Two types of specimens were prepared: thin films made by electrolytic polishing and "lamellas" made in the FIB device. Observations were made on transmission electron microscopes JEM200CX and Tecnai.

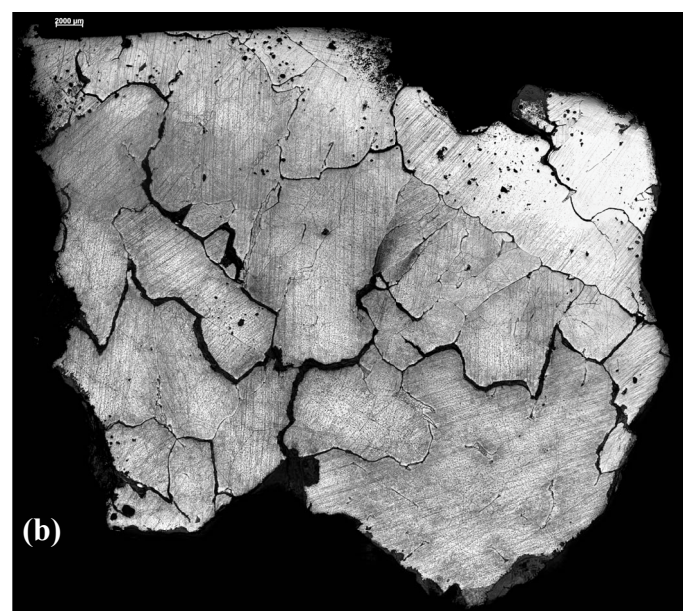
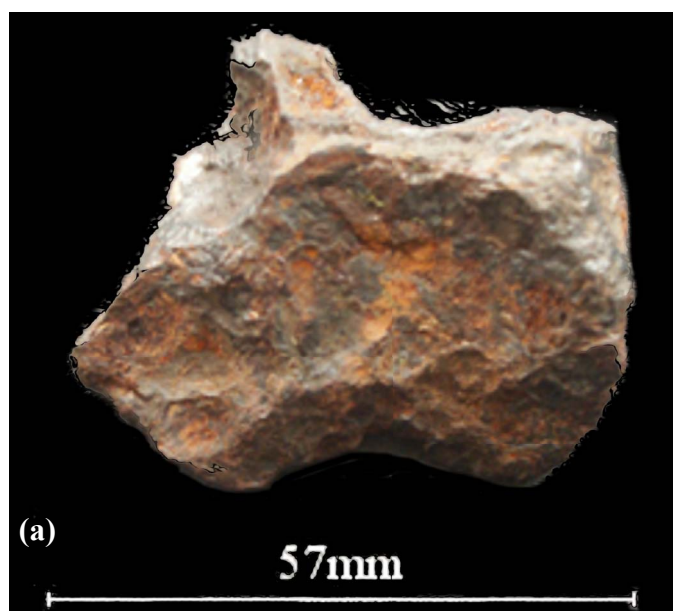


Fig. 2. Investigated meteorite from Morasko craters (a). Weight 260 g, dimensions: approx. 56×42×44 mm, regmaglipts 18-34×3-6 mm. Macro-structure of the cross-section of the meteorite (b)

2.1. Microstructure research

Initial investigations of the meteorite structure were made on a light microscope and a scanning electron microscope. A typical image of the structure observed on LM light microscopy is shown in Fig. 3. The main components of the structure are the Neumann bands, occurring on the background of the kamacite matrix. They are arranged in various crystallographic systems. Grains with one, two or three systems are observed. The density of bandwidth determined by the secant method varies from 6.2-17.3 mm⁻¹. Next to the Neumann bands, rhabdite sections were visible (Fig. 3a,b).

The test sample also sporadically found the presence of a plessite (Fig. 3c) and austenitic-martensitic islands (Fig. 3d). Structural identification has been confirmed by studies on SEM. Fig. 4a shows the crystals of rhabdite, and Fig. 4b shows carbides. The concentration of nickel in the kamacite matrix was about 6.7%, in the taenite from the plessite – about 32%, and in the austenitic-martensitic islands about 25%.

2.2. Studies of dislocation structure of matrix

The basic aim of the research was to analyze the dislocation structure of the meteorite. The structure of the metallic matrix (morphology, dislocation density, crystallography) as well as the structure of Neumann bands (crystallographic relations, morphology) were examined.

The dislocation structure of the kamacite matrix containing about 7% Ni is very diverse, both in terms of morphology and dislocation density. Examples of structures at various locations in the sample are shown in Fig. 5. Dislocation density ρ_d estimated after taking into account some dislocations invisible for a given warp orientation ($\bar{g} \cdot \bar{b} = 0$), ranged from 10⁹ cm⁻²

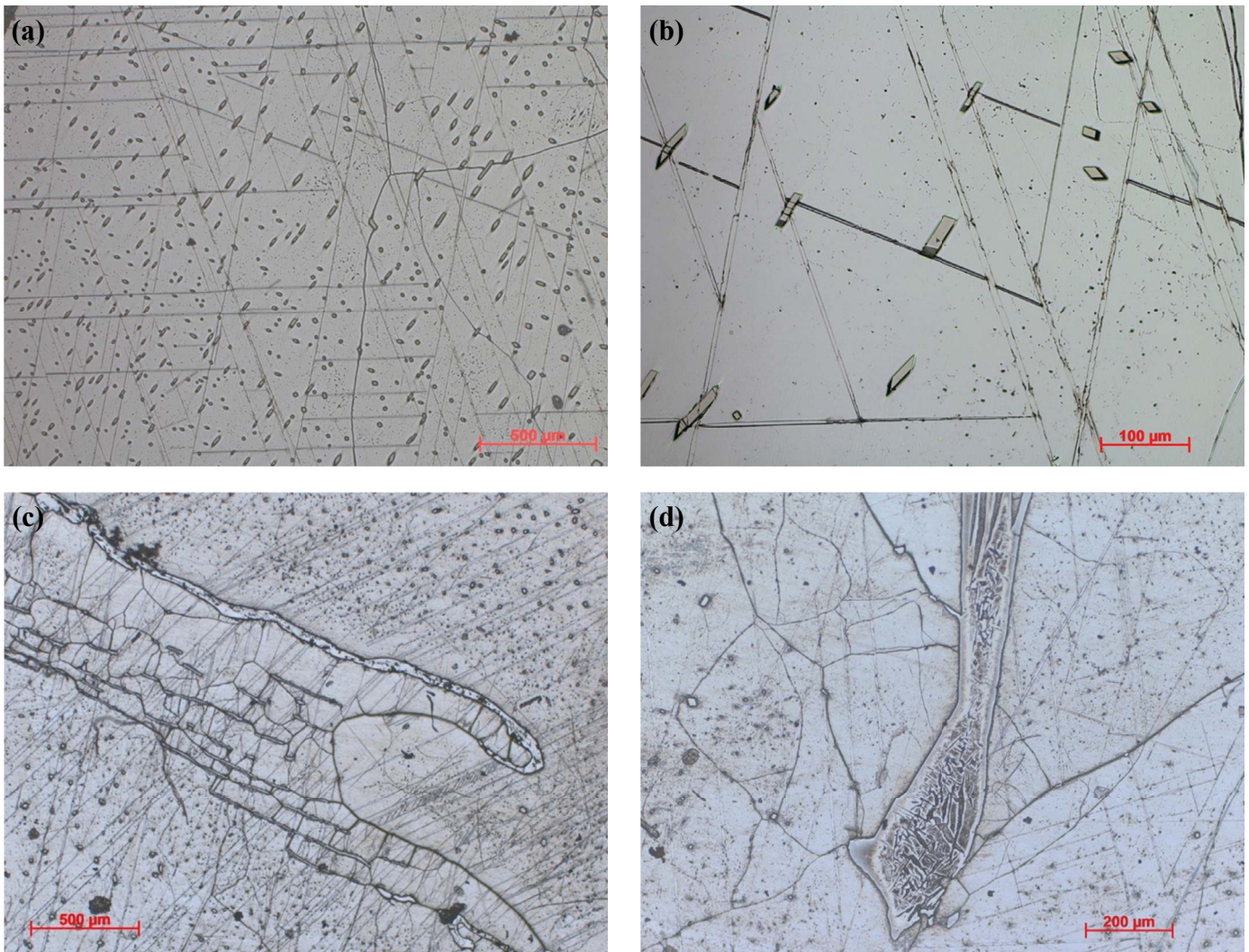


Fig. 3. Meteorite microstructure under Light Microscopy (LM); (a, b) a general view, (c) plessite, (d) austenitic-martensitic island

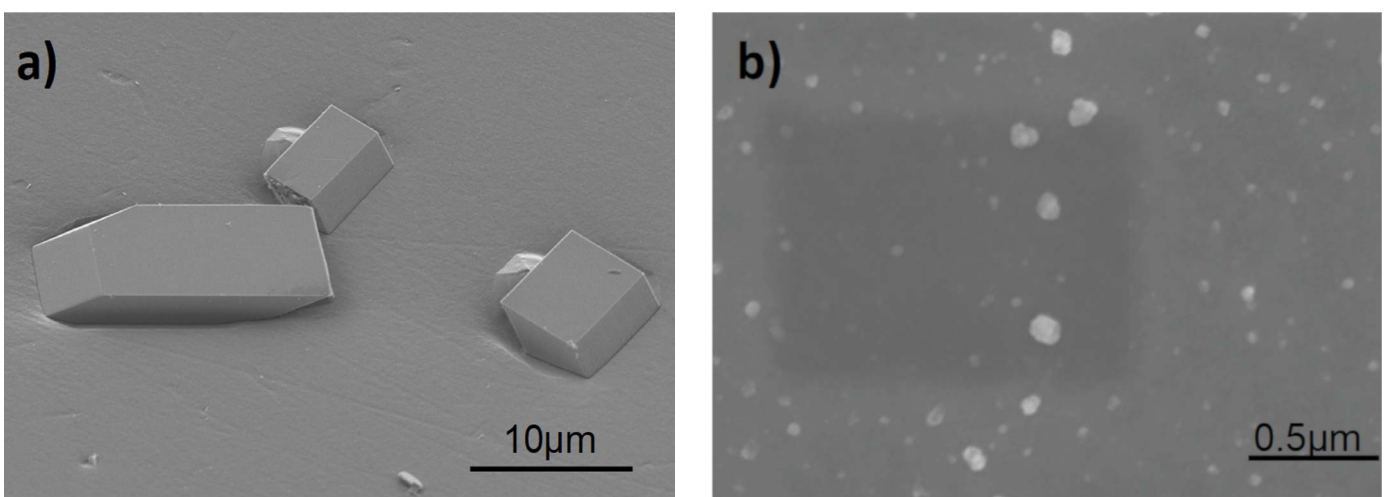


Fig. 4. Meteorite microstructure under Scanning Electron Microscopy (SEM): (a) iron-nickel phosphide, (b) MC, M_3C carbides

to 10^{11} cm^{-2} . In areas of low density ρ_d dislocation lines have an identical crystallographic orientation – they lie on the same plane, along the direction of the type $\langle 111 \rangle$ and have the same Burgers vector (Fig. 5a,b,c). They can be classified as screw

dislocations. In other areas where the density of dislocations is much larger, dislocations are tangled and their images overlap (Fig. 5d). Dislocations lie on different planes and have different Burgers' vectors.

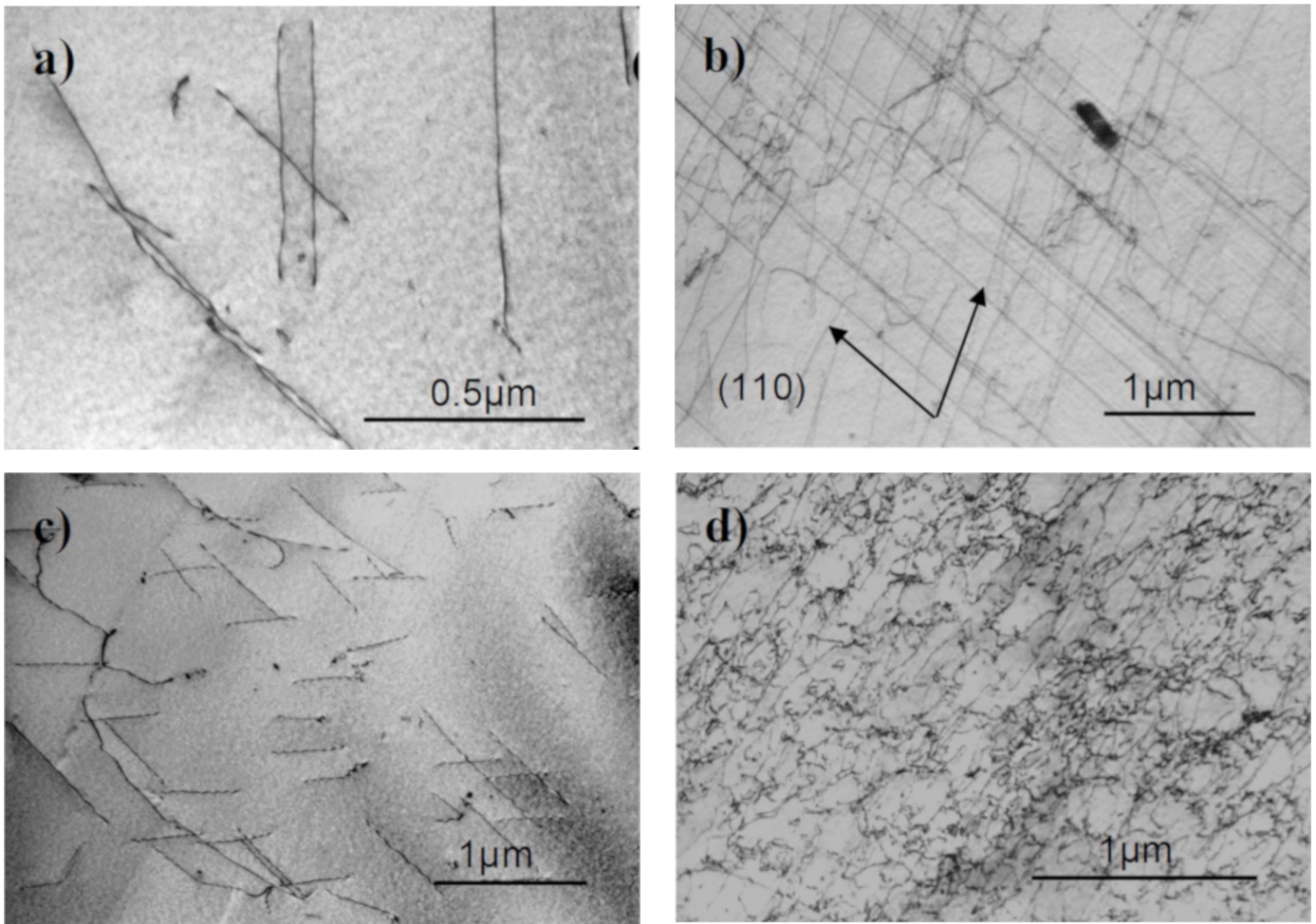


Fig. 5. Dislocation structure of ferritic matrix (kamacite) in various places on the specimen; a) $\rho = 2.1 \times 10^9 \text{ cm}^{-2}$, b) $\rho = 9 \times 10^9 \text{ cm}^{-2}$, c) $\rho = 1.2 \times 10^9 \text{ cm}^{-2}$, d) $\rho = 4 \times 10^{10} \text{ cm}^{-2}$

In the kamacite grains, moreover, many areas are polygonised, with low-angle boundaries with a disorientation angle of 0.25° . Examples of such areas are shown in Fig. 6.

2.3. Neumann band structure research

The Neumann bands were in the form of regular plates with a thickness of $0.5\text{-}2 \mu\text{m}$, typical deformation twins in the fcc lattice alloys [16]. Examples of twins forming the Neumann bands are shown in Fig. 7. The twin plane was the $\{211\}$ type

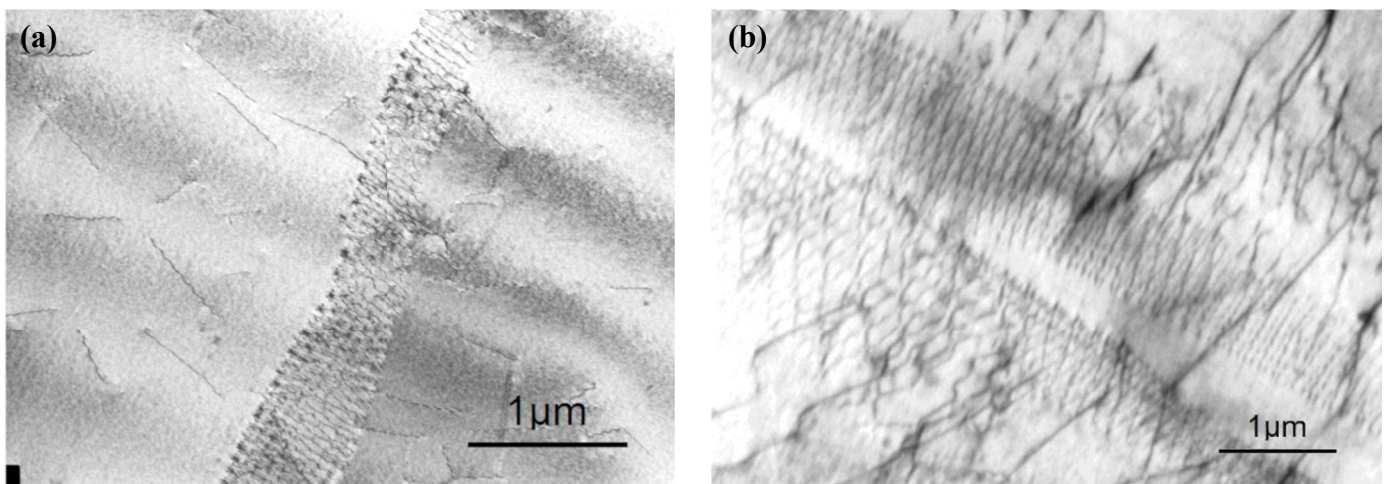


Fig. 6. Low-angle boundaries

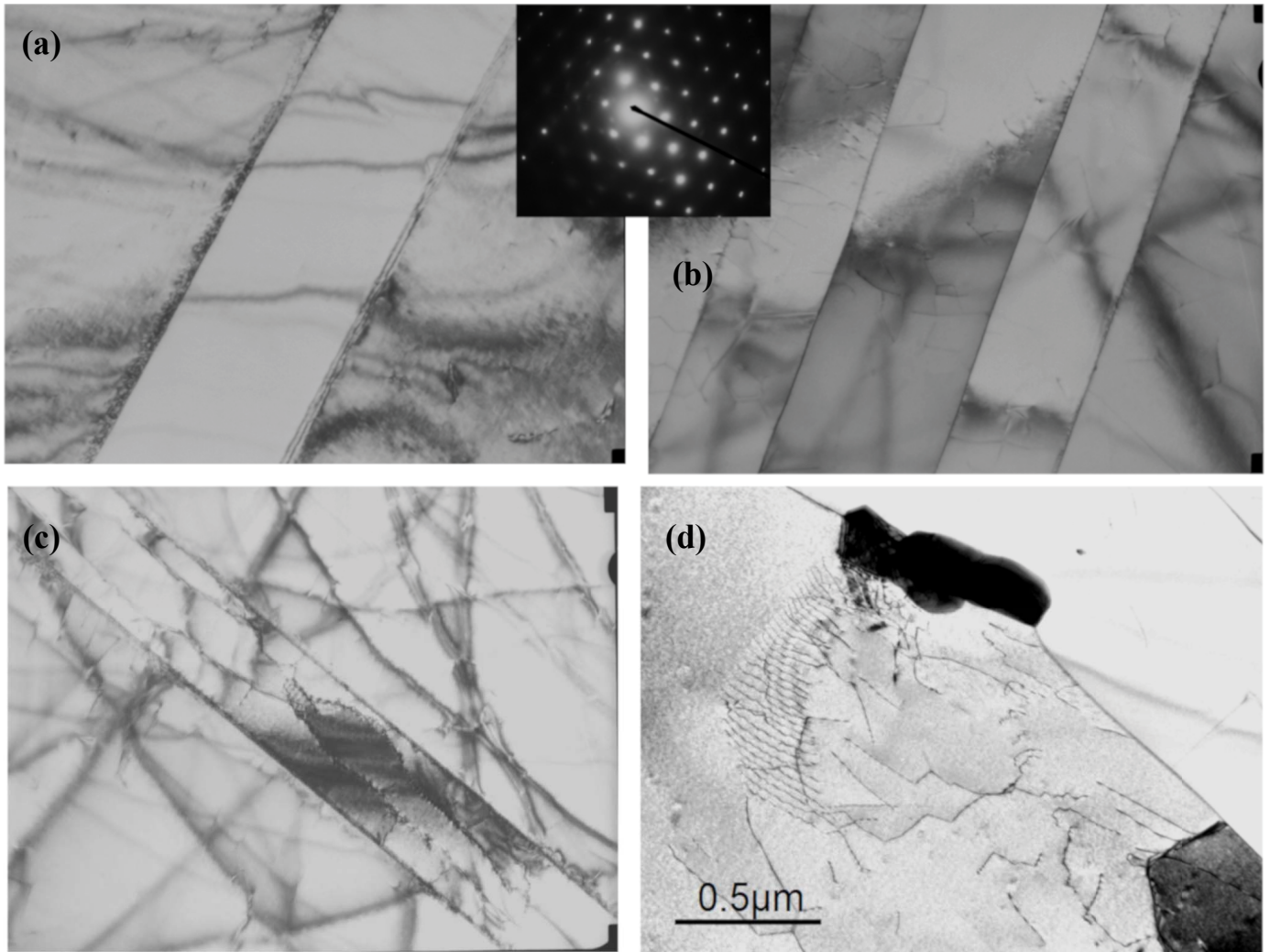


Fig. 7. Typical Neumann bands (deformation twins): (a) single band, (b) double band, (c) polygonised band, (d) carbides lying on the twin boundary

plane. In Fig. 7b there are two bands lying very close to each other, with crystallographic parameters identical to those in Fig. 8a. When observed on a light microscope these two bands are indistinguishable, we see them as a single band. There were cases where the interior of the band was polygonised (Fig. 7d).

Twin boundaries could also interact with carbide precipitates. The stresses occurring at this point caused the formation of sub-boundaries (Fig. 7e).

In the dislocation structure of the examined meteorite, deformation of the bands was observed (Fig. 8), and their dis-

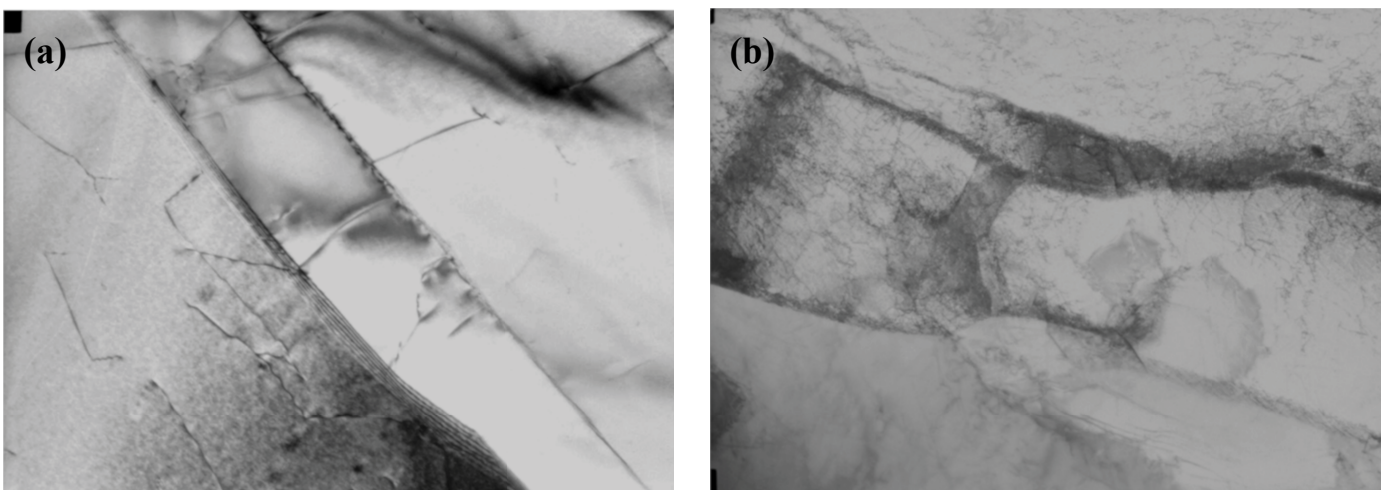


Fig. 8. Deformed Neumann's bands

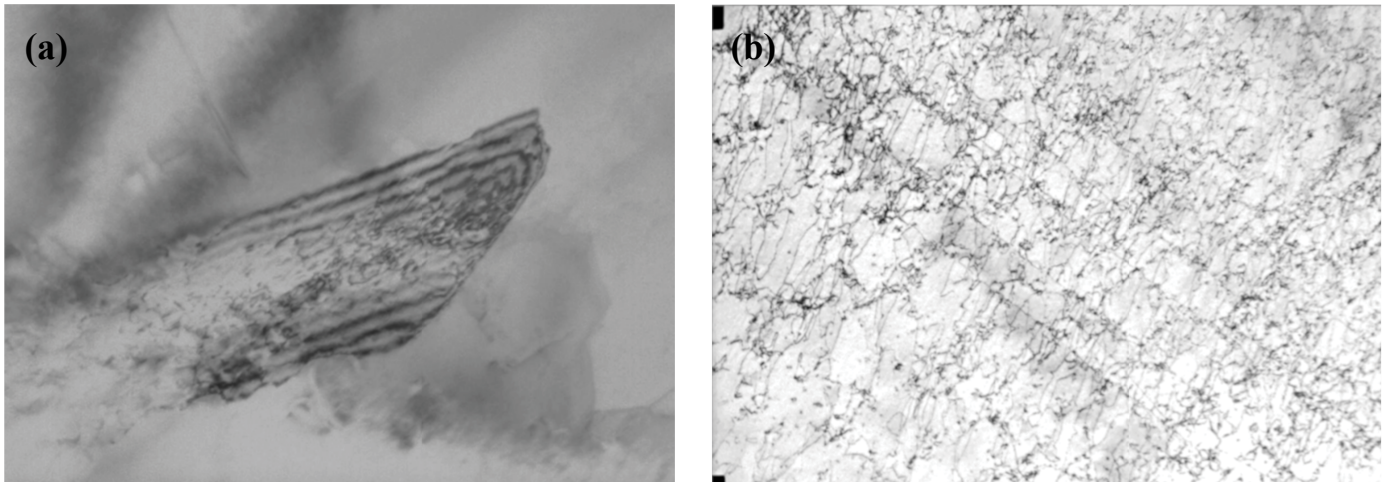


Fig. 9. The disappearance of Neumann's bands

appearance (Fig. 9). The band shown in Fig. 8a is deformed – its width changes and the twin boundaries cease to be parallel, however it still remains in the twin orientation with the matrix. Many bands are narrowing (Fig. 8b). An increase in dislocation density inside the (twin) band and on its borders is observed.

The disappearance of twins is shown in Fig. 9a. The retained fragment of the Neumann band still stays in twin orientation with the matrix and is built of elongated areas separated by boundaries, mostly low-angle ones. In places where the bands have disappeared, one can sometimes observe a directed increase in dislocation density (Fig. 9b).

In the structure also bands without twin orientation are present, which are classified as slip bands. A typical example of such a band is shown in Fig. 10.

A more complex structure is shown in the band shown in Fig. 10b. Here the band boundaries are wide-angle, and inside them there are many subgrains with low-angle boundaries and high dislocation density. Some parts of the band retain twin orientation with the matrix. These bands are indistinguishable by light and scanning electron microscopy from twin bands.

3. Summary

The observed structural components are evidence of strong primary segregation of the Fe-Ni alloy, crystallization in extremely low temperature gradient and the inability to homogenize the alloy. Phase transformations $\gamma - \alpha$ takes place under slow cooling conditions, moreover, local formation of martensite takes place after crossing the M_s line of the system.

The research results show that the conditions accompanying meteors and iron meteorites have the strongest influence on the dislocation structure. There is a constant evolution of this structure caused by the stress field: formation of free dislocations, dislocation systems, Neumann bands and slip bands. Deforming at low and relatively higher temperatures results in Neumann bands, slip bands, and the dislocation structure of the matrix are single screw dislocations and dislocation tangles.

The Neumann bands are the deformation twins in the form of 0.5-2 nm plates, with the twin plane $\{211\}$. The following are noted: the variation of the twin boundaries structure, dislocation density inside the twins, polygonisation and disappearance of bands. The disappearing Neumann bands form traces in the form

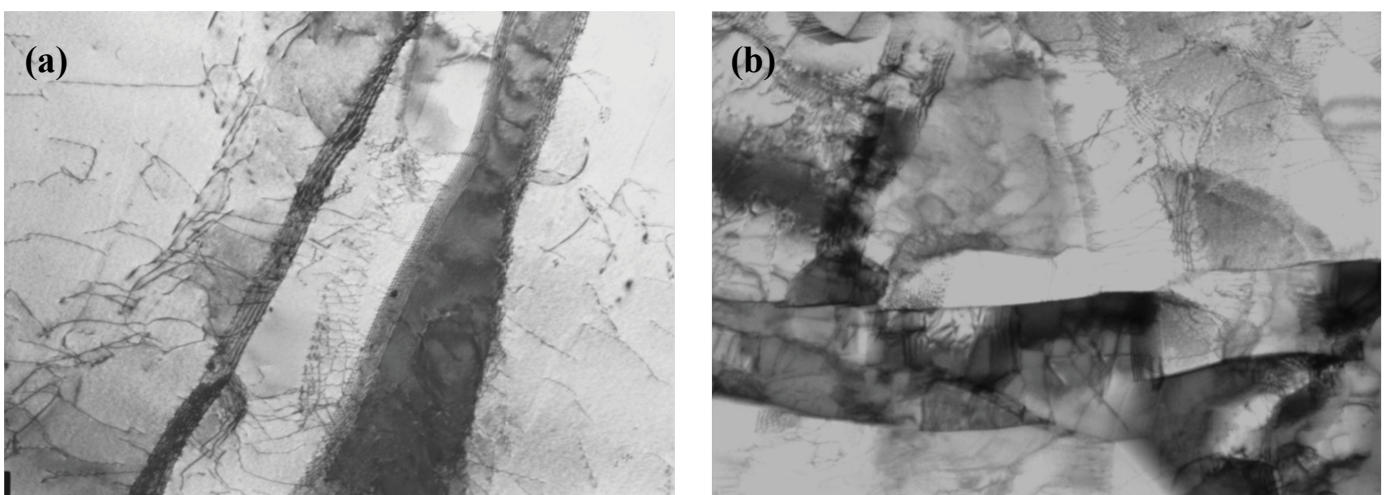


Fig. 10. Deformation bands

of directed areas with a higher dislocation density ρ_d . In addition to the Neumann bands, the structure consists of slip bands, separated by high-angle boundaries, with subgrains and a high density of dislocations, locally in a twin relation with the matrix.

Acknowledgements

The work was realized as a part of fundamental research financed by AGH University of Science and Technology project number 16.16.110.663.

Participation in the conference was financed under project POWR.03.05.00-00-Z307/17-00. The authors thank Mr. Krzysztof Socha for making the meteorite available for research.

The publication was financed by the Ministry of Science and Higher Education under project 844/P-DUN/2019 zad. 2



REFERENCES

- [1] T. Rehren, T. Belgys, A. Jambon, G. Káli, Z. Kasztovszky, Z. Kis I. Kovács, B. Maróti, M. Martín-Torres, G. Miniacif, V.C. Pigott, M. Radivojević, L. Rosta, L. Szentmiklósi, Z. Szőkefalvi-Nagy, 5,000 years old Egyptian iron beads made from hammered meteoritic iron, *Journal of Archaeological Science* **40**, 4785-4792 (2013).
- [2] D. Comelli, M. D'Orazio, L. Folco, M. El-Halwagy Frizzi, T. Alberti, R. 4, Capogrosso V., Elnaggar A., Hassan H., Nevin A., Porcelli F. 7, Rashed M.G., Valentini G., The meteoritic origin of Tutankhamun's iron dagger blade, *Meteoritics & Planetary Science* 1-9 (2016).
- [3] A. Kotowiecki, Artifacts in Polish collections made of meteoritic iron; *Meteoritics & Planetary Science* **39**, 151-156 (2004).
- [4] J. Piaskowski, A study of the origin of the ancient highnickel iron generally regarded as meteoritic. In *Early Pyrotechnology: the evolution of the first Fire-using Industries*, edited by Wertime T. A. and Wertime S. F. Washington, D.C.: Smithsonian Institute 237 (1982).
- [5] R. Błoniarz, I. Suliga, Struktura i własności próbek meteorytów żelaznych poddanych eksperymentalnej przeróbce plastycznej na gorąco, *Zeszyty Studenckiego Towarzystwa Naukowego* edited by L. Kurcz, A. Gołdasz (red.), Artykuły laureatów 50. Sesji Studenckich Kół Naukowych Pionu Hutniczego Akademii Górniczo-Hutniczej, 41, Kraków 2013.
- [6] K. Socha, I. Suliga, H. Krawczyk, Meteoryty – najstarszy materiał do wytwarzania narzędzi żelaznych? (Meteorites – the oldest material for fabricating iron artifacts), *Acta Societatis Metheoriticae Polonorum* **5**, 104 (2014).
- [7] Riley, *Journal of the Iron and Steel Institute*, 1889.
- [8] V.F. Buchwald, *Handbook of Iron Meteorites*, Univ. of California Press, 1975.
- [9] R.A. Jago, A structural investigation of the Cap York meteorite by transmission electron microscopy, *Journal of Materials Science* **9**, 564 (1974).
- [10] C.S. Smith, Metallographic study of metals after explosive shock, *Transaction of AIME* **212**, 574 (1958).
- [11] C.S. Barret, B. Massalski, *Structure of Metals. Crystallographic Methods. Principles and Data*, Mc Graw Hill, 1966.
- [12] M. Popławski, K. Józwiak, T. Kachlicki, Badania metalograficzne i mikroanalityczne meteorytu Morasko, *Metallography and Microanalysis Study of the Morasko Meteorite, Acta Societatis Metheoriticae Polonorum* **2**, 117-124 (2011).
- [13] J. Pokrzywnicki, I. Meteorites of Poland. II. Catalogue of Meteorites in the Polish Collection. *Studia Geologica Polonica, Warszawa* **15**, 1-176 (1064).
- [14] B. Dominik, Shock and thermal transformation in meteorites from the Morasco, crater field, *Meteoritics* **12**, 207 (1978).
- [15] M. Szurgot, K. Roźniakowski, T. Wojtatowicz, K. Polański, Investigation of Microstructure and Thermophysical Properties of Morasco Iron Meteorites, *Crystal Research and Technology* **43**, 921 (2008).
- [16] W. Osuch, *Bliźniaki przemiany w stalach niskowęglowych*, Wydawnictwa AGH, Kraków 2010.